JOURNAL OF GEOPHYSICAL RESEARCH, VOL. 113, C07049, doi:10.1029/2007JC004707, 2008

Physical and chemical signatures of a developing anticyclonic eddy in the Leeuwin Current, eastern Indian Ocean

Harriet L. Paterson,[1] Ming Feng,[2] Anya M. Waite,[1] Damià Gomis,[3] Lynnath E. Beckley,[4] David Holliday,[4] and Peter A. Thompson[5]

Received 20 December 2007; revised 5 May 2008; accepted 20 May 2008; published 30 July 2008.

[1] A multidisciplinary cruise aboard the R/V *Southern Surveyor* was conducted in May 2006 to sample a developing anticyclonic eddy of the Leeuwin Current off Western Australia. The eddy formed from a meander of the Leeuwin Current in mid-April 2006 and remained attached to the current until mid-August. In this study, a combination of satellite data (altimeter, sea surface temperature, and chlorophyll *a*) and shipboard measurements (acoustic Doppler current profiler and conductivity-temperature-depth) were used to characterize the physical and chemical signatures of the eddy. The temperature-salinity properties of the mixed layer waters within the anticyclonic eddy and on the shelf were both connected to that of the Leeuwin Current, indicating the water mass in the eddy is mainly derived from the Leeuwin Current and the modified Leeuwin Current water on the shelf. Above the salinity maximum near the eddy center, there was a regionally significant concentration of nitrate (>0.9 μmol L^{-1}), and the maximum (2 μmol L^{-1}) was at 150 m depth, below the photic zone. Nitrification within the eddy and/or local upwelling due to the forming eddy could be responsible for this high concentration of nitrate near the eddy center, which potentially makes the eddy a relatively productive feature in the Leeuwin Current.

Citation: Paterson, H. L., M. Feng, A. M. Waite, D. Gomis, L. E. Beckley, D. Holliday, and P. A. Thompson (2008), Physical and chemical signatures of a developing anticyclonic eddy in the Leeuwin Current, eastern Indian Ocean, *J. Geophys. Res.*, *113*, C07049, doi:10.1029/2007JC004707.

1. Introduction

[2] Mesoscale eddies are important in redistributing the momentum, heat, salt and biochemical tracers in the ocean. The west coast of Australia is a unique region to study the role of mesoscale eddies, as this region has the highest eddy kinetic energy of all eastern boundary systems [*Feng et al.*, 2005]. The Leeuwin Current (LC) flows poleward along the continental shelf break because of the anomalous pressure gradient in the eastern Indian Ocean [*Cresswell and Golding*, 1980]. The LC is highly unstable during the austral autumn-winter season when the current is at its peak strength, and both anticyclonic and cyclonic eddies are formed from the current. *Pearce and Griffiths* [1991] proposed that anticyclonic eddies (typically warm core) were developed from the LC primarily by interactions with cyclonic eddies seaward of the current. The resulting anticyclonic eddies have been demonstrated to entrain productive shelf waters [*Pearce and Griffiths*, 1991; *Feng et al.*, 2007], contain coastal phytoplankton communities [*Moore et al.*, 2007], and have higher level of chlorophyll *a* biomass [*Griffin et al.*, 2001; *Moore et al.*, 2007; *Feng et al.*, 2007].

[3] In October 2003, a mature anticyclonic/cyclonic eddy pair, which developed from a meander structure of the LC in May 2003 and detached in late August/early September 2003, was investigated [*Waite et al.*, 2007a]. The anticyclonic eddy had an anomalously high concentration of healthy coastal diatoms which were thriving in a low-nutrient and deep mixed layer (~275 m) environment [*Thompson et al.*, 2007]. Survival of diatoms under these conditions was attributed to vertical migration and high mixing rates within the eddy [*Thompson et al.*, 2007]. *Waite et al.* [2007a] hypothesized that these coastal diatoms were incorporated into the eddy during its formation in May 2003, and required about 1 μmol L^{-1} of initial nitrate concentration to sustain their growth over the subsequent months. Using a 1-D model simulation, *Greenwood et al.* [2007] concluded that initial nitrate injection during the formation of the anticyclonic eddy may account for up to 75% of the primary production as it migrates offshore. In addition, they suggested that the very deep mixed layer generated by these eddies may increase the residence time of sinking particles, increasing the importance of regenerated nutrients. Other potential mechanisms, e.g. regional

[1] School of Environmental Systems Engineering, University of Western Australia, Nedlands, Western Australia, Australia.
[2] CSIRO Marine and Atmospheric Research, Wembley, Western Australia, Australia.
[3] Institut Mediterrani d'Estudis Avançats, UIB-CSIC, Esporles, Spain.
[4] School of Environmental Science, Murdoch University, Murdoch, Western Australia, Australia.
[5] CSIRO Marine and Atmospheric Research, Hobart, Tasmania, Australia.

0148-0227/08/2007JC004707$09.00

subduction, nitrogen fixation, and exchanges with other eddy features, were also suggested to contribute to the nitrogen balance within the eddy.

[4] Characterization of the nutrient climatology of the Leeuwin Current has only recently been undertaken [*Lourey et al.*, 2006]. In general, it was found that the surface waters were low in nitrate (<0.5 μ mol L^{-1}), largely devoid of phosphate but contained reasonably high levels of silicate (4 μ mol L^{-1}). *Twomey et al.* [2007] described the nutrient regime of the surface waters of the Leeuwin Current during the spring-summer season as nitrate impoverished with low phytoplankton biomass. They also found that production is fuelled by microbial regeneration and nitrogen fixation was unimportant during this season.

[5] In order to investigate the nutrient hypothesis described by *Greenwood et al.* [2007] and *Waite et al.* [2007a], an R/V *Southern Surveyor* cruise was undertaken in May 2006 to sample a developing anticyclonic eddy from the LC meander. The physical and chemical signatures of the eddy is reported in this paper, and compared with the mature anticyclonic eddy investigated in 2003 [*Feng et al.*, 2007; *Waite et al.*, 2007a].

2. Methods

[6] From April 2006, mesoscale structures in the LC were monitored using sea surface temperature (SST) images supplied by the CSIRO Marine and Atmospheric Research Remote Sensing Facility, daily surface current analysis from the CSIRO BLUELink project http://www.cmar.csiro.au/remotesensing/oceancurrents), and the Naval Research Laboratory nowcast model output supplied by the Asia Pacific Data Research Center in University of Hawaii. These data identified the development, and subsequent detachment, of an anticyclonic eddy that was studied in situ during May 2006; this eddy will be referred to as Alpha. In this study, weekly sea surface height anomalies (SSHA) based on the combined TOPEX Poseidon (Jason-1) and ERS-1/ERS-2 (Envisat) satellite missions, obtained from CLS Space Oceanography Division (hereafter referred to as Aviso SSHA) [*Le Traon et al.*, 1998; *Ducet et al.*, 2000], were used to follow the formation and movement of Alpha.

[7] The R/V *Southern Surveyor* cruise sampled the anticyclonic eddy Alpha during the period 2–28 May 2006 (Figure 1). A shipboard acoustic Doppler current profiler (ADCP) (Teledyne RD Instruments) measured the ocean currents from 23 to about 400 m depth in 8 m bins. A total of 134 conductivity-temperature-depth (CTD) stations were occupied using a Seabird SBE 9/11 dual-sensor unit and a Chelsea TGI fluorometer (Aanderaa Oxygen Optode [716]). The temperature, salinity, fluorescence and oxygen were measured from the sea surface through the water column to about 500 m or just above the seafloor at most stations. Water samples for nutrients were taken at standard depths for most CTD stations (surface, 25, 50, 100, 150, 200, 300, 400, 500 m). The CTD data were used to characterize the temperature-salinity relationship in the region and determine the depth of the mixed layer. The mixed layer depth was defined with a $0.125\sigma_\theta$ increment from 10 m depth.

[8] Meteorological conditions were measured by onboard instrumentation during the cruise. Estimates of short and long wave radiation data along with sensible and latent heat were also obtained from National Center for Environment Prediction (NCEP) [*Kalnay et al.*, 1996]. The data were used to calculate the daily and monthly mean air-sea heat fluxes for the eddy region. Twelve NCEP data points were used, in the domain of 110.6°E–114.3°E and 29.5°S–35.2°S.

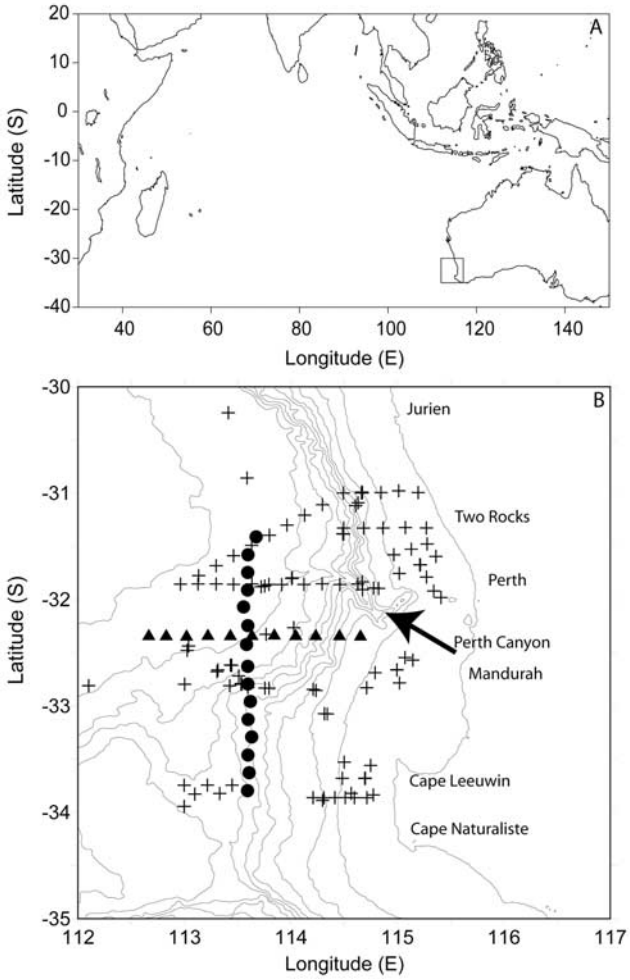

Figure 1. Station locations and bathymetric contours (500 m depth intervals) for the study area off southwestern Australia in May 2006. Solid circles represent conductivity-temperature-depth probe (CTD) stations along the 113.6°E transect, and solid triangles are CTD stations along the 32.3°S transect. Crosses indicate all other stations.

[9] To calculate the horizontal and vertical current velocities, we used the method described by *Gomis et al.* [2001]. This consists of a multivariate analysis of CTD and ADCP observations that yields gridded fields of dynamic height and velocity. In order to reduce the impact of the lack of synopticity of the data set on some of the computations (e.g., on the spatial analysis and the subsequent computation of the vertical velocity), the overall data set was divided into three subsets, as indicated in Table 1. Stations 55–69 were discarded because they were obtained far away from their neighbors in time (or conversely, all the stations in their vicinity were obtained with a time lag of more than one week). The first data subset consists of stations 1–54 (obtained between 2–11 May), of which stations 39–49

Table 1. Spatial and Temporal Distribution of Oceanographic Stations During the May 2006 Research Cruise[a]

Subset	Dates	CTD Casts	ADCP Profiles	Domain
1	02–11 May 2006	1–54	1–1309	−33°S < lat < −31°S 113°E < lon < 115°E
Not considered	12–13 May 2006	55–69	1310–1586	- - -
2	14–25 May 2006	70–134	1587–3193	−34°S < lat < −32°S 113°E < lon < 115°E

[a]The survey was separated into three subsets, of which only two were considered to solve the Omega equation. CTD, conductivity-temperature-depth probe; ADCP, acoustic Doppler current profiler; lat, latitude; lon, longitude.

corresponded to a west-east transect passing to the north of the eddy center. The second data subset consists of stations 70–134 (obtained between 14–25 May), of which stations 110–116 and 119–126 corresponded to a north-south transect passing just east of the eddy center (Figure 1). In the analysis, the correlation scale was set to 20 km, noise-to-signal ratios were 0.001 for the CTD data and 0.01 for the ADCP data. The separation distance between the CTD transects was rather large (~60 km), though the data distribution was improved significantly when considering the ADCP data. Hence, the output fields were smoothed by setting the cutoff wavelength to 100 km.

[10] A preliminary exploration of the density structure showed that most of the baroclinic structure was confined within the upper 500 m. In fact, current velocities measured by ADCP were rather weak below 400 m, confirming that 500 m could be reasonably taken as a no-motion level. Therefore, the multivariate analysis was performed considering a quasi-geostrophic (QG) balance between dynamic height referred to 500 m and actual ADCP velocities. The presence of a barotropic velocity was not explored in detail, but the low-velocity values measured below 400 m indicate that the eventual barotropic component should be lower than 5 cm s^{-1}.

[11] Vertical velocities were computed from the dynamic height field using the QG Omega equation [*Holton*, 1992]. We set $w = 0$ at the upper (z = 0) and lower (z = 500 m) boundaries of the 3D domain, whereas at the lateral boundaries we used Neumann conditions ($\partial w/\partial n = 0$). Provided the horizontal scale of the structures is smaller than the size of the domain, the ellipticity of the Omega equation ensures that the interior solution for w is relatively insensitive to the imposed conditions [see *Gomis and Pedder*, 2005a, 2005b]. More problematic is the eventual effect of the lack of synopticity of the data. *Gomis and Pedder* [2005a, 2005b] have shown that when surveying a propagating structure as

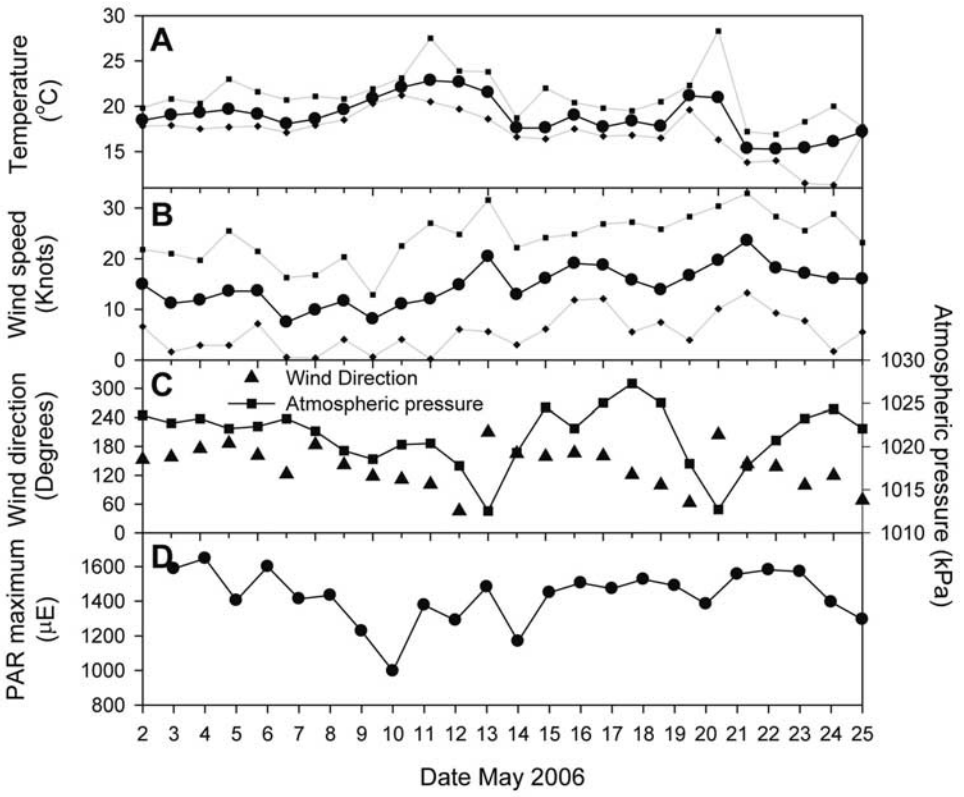

Figure 2. Summary of daily meteorological conditions from 2–27 May from shipboard instrumentation. (a) Air temperature (°C) average, maximum, and minimum; (b) wind speed (knots) average, maximum, and minimum; (c) average wind direction (degrees) and average atmospheric pressure (kPa); and (d) maximum photosynthetic available radiation (μE).

the one dealt with in this work, the uncertainty in the vertical velocity could be easily of the order of 30–50% of the obtained values.

3. Results

3.1. Meteorology

[12] The passages of two low-pressure systems on 14 and 22 May dominated the weather during the voyage (Figure 2). Prior to the low-pressure systems, the daily mean air temperatures rose to 23°C and 21°C, respectively, and dropped to 18 and 15°C afterward. The average wind speeds varied between 10 to 20 knots, with slight increases during and after the passages of the depressions. At the beginning of the cruise and during the passage of depressions the wind direction was southerly, and at all other times it tended to be more easterly. The maximum daily photosynthetically available radiation was ~1400 μE for most of the month, except around 10 May.

3.2. Satellite Observations

[13] In mid-April 2006 (not shown), the LC, identified by warm water (>22°C), formed a large anticyclonic meander, with a center at approximately 32°S, 114.8°E. During the next few weeks this meander developed into an eddy-like structure, with a positive sea surface height anomaly located shoreward of its geometric center. From early May, the anticyclonic feature (Alpha) could be detected by Aviso SSHA, SST and chlorophyll *a* (Figures 3 and 4). Note that another anticyclonic eddy had formed from the LC in March 2006 at the same location, which detached and moved into the open ocean in early April 2006.

[14] During the cruise period, Alpha was the dominant mesoscale feature in the region off Perth and had a strong connection with the LC and shelf waters near 32°S. To the north of the eddy, cooler Subtropical surface water (STSW) with a negative sea surface height anomaly moved shoreward and developed into a weak, cyclonic structure. There was another, but weaker, cyclonic structure (Beta) distinguished by negative SSHA to the east of Alpha (Figure 3).

[15] The boundary of Alpha, as identified by high sea surface temperature, changed over the 27 days of the cruise. Initially, the eddy was elliptical with its north-south extent being almost twice its east-west extent (Figure 5a). This elliptical shape was short-lived, and on 17 May it became more circular, with a weak elliptical shape in the east-west direction (Figure 5).

[16] The movement of Alpha was estimated by identifying the geometric center of the eddy using daily SST images and the peak sea surface height from weekly Aviso SSHA data. The daily SST images indicated that the eddy remained roughly stationary over the two periods, 2–15 May and 18–28 May (Figure 5a), with the transition coinciding with the time the eddy changed its shape. It propagated a total of 80 km during the study period. There is a 50 km difference between the distances traveled by the eddy using SST and SSHA data as the initial estimations of the center from SSHA were 67 km shoreward of those determined from SST images. We note that SSHA data from the shelf region may be unreliable because of the shallow waters, so that the position of the eddy determined from satellite altimeter data could have an error as large as 50 km,

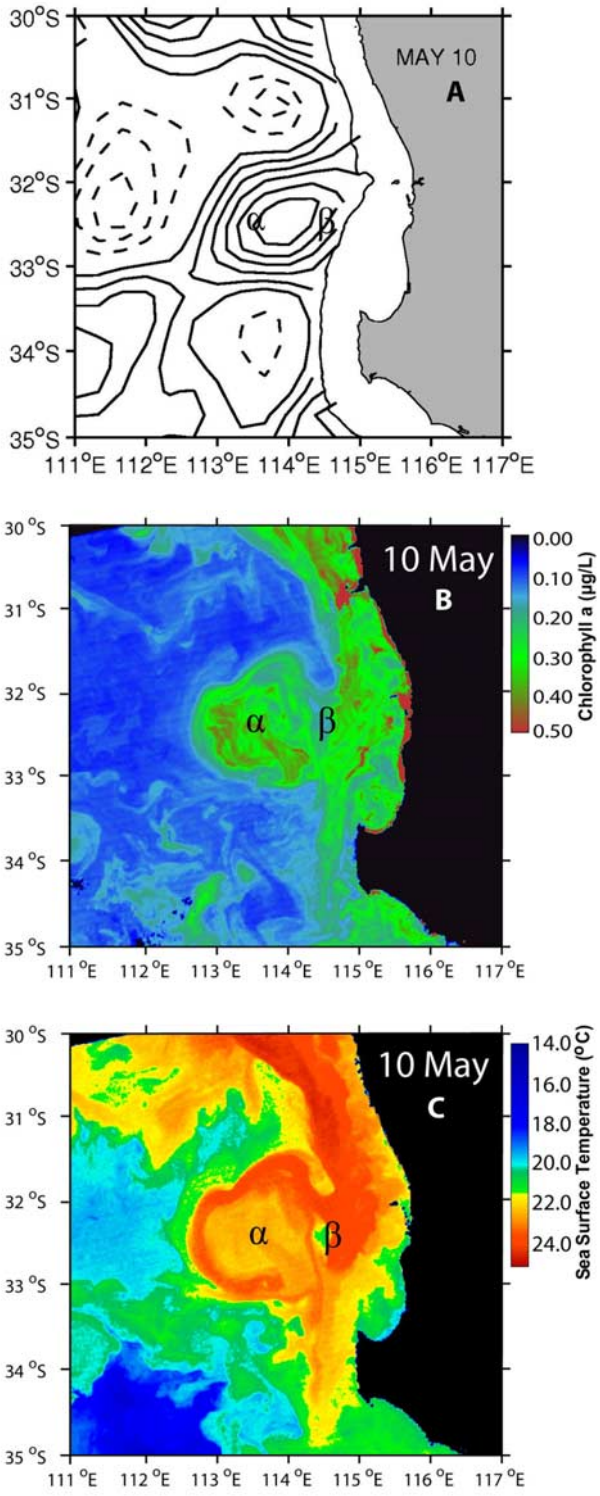

Figure 3. (a) Sea surface height anomaly off southwestern Australia on 10 May 2006. Contours are at 5 cm intervals, and the 200 m bathymetry contour is also shown. (b) Sea surface chlorophyll a concentrations and (c) sea surface temperatures, both from Moderate Resolution Imaging Spectroradiometer (on EOS) (MODIS) aqua, on 10 May 2006. The α and β annotations in Figures 3b and 3c identify the anticyclonic study eddy and the associated small cyclonic eddy, respectively.

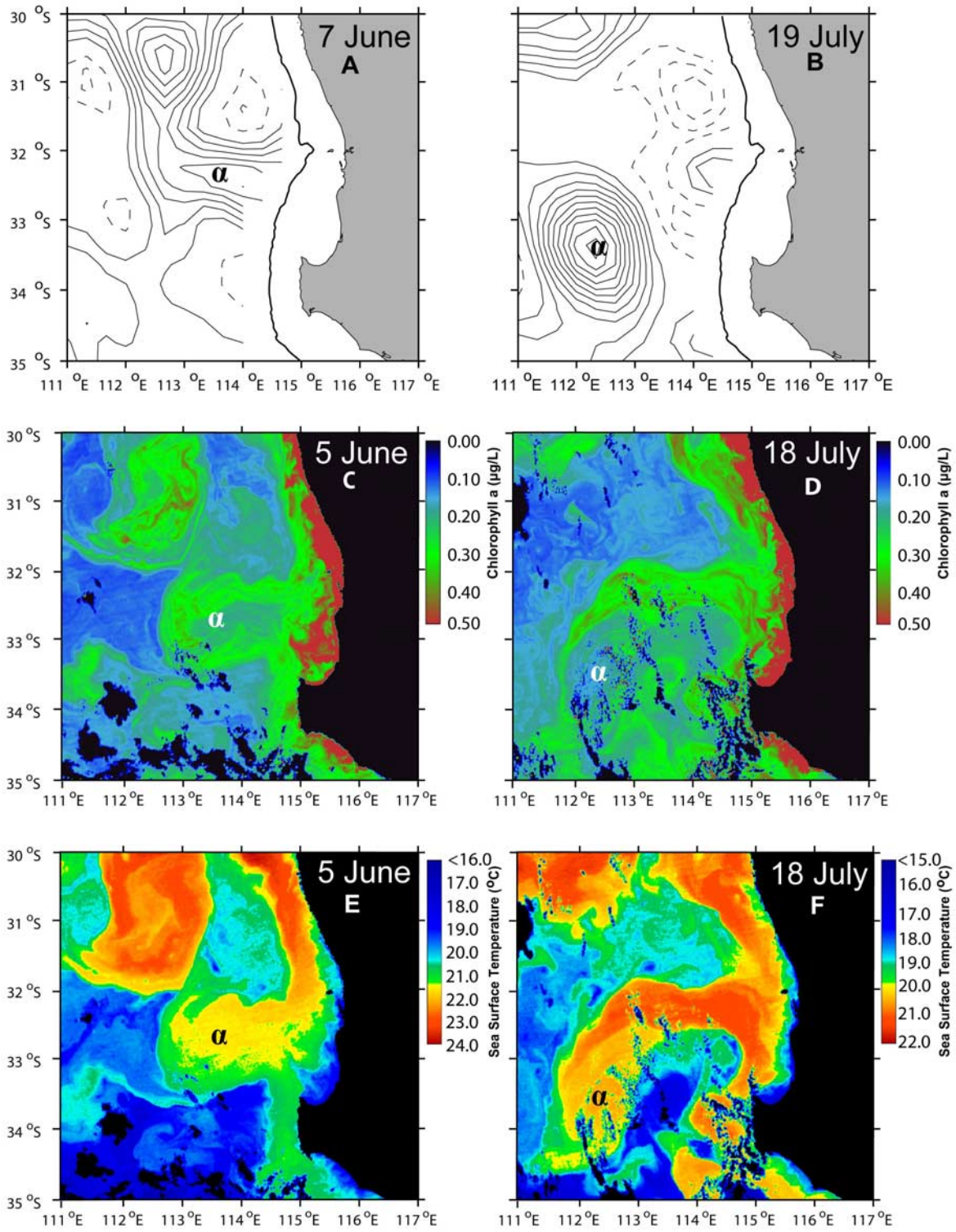

Figure 4. (a, b) Sea surface height anomalies off southwestern Australia at 5 cm intervals on both 7 June and 19 July 2006. The 200 m bathymetry contour is also shown. (c, d) Sea surface chlorophyll *a* concentrations and (e, f) sea surface temperatures, both from MODIS Aqua satellite, on 5 June and 18 July 2006. The α on plot identifies the anticyclonic eddy.

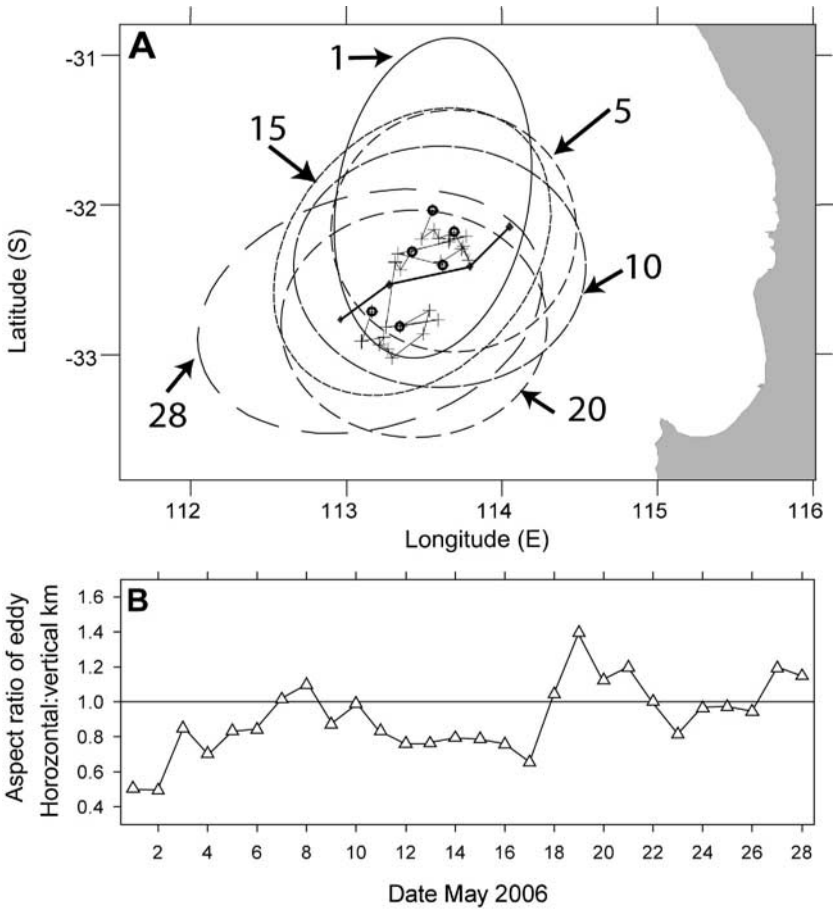

Figure 5. Estimation of eddy size, aspect ratio, and geometric center off southwestern Australia. (a) (plus signs) Lagrangian tracks of the geometric center of the eddy daily from 1–28 May 2006; geometric center locations on 1, 5, 10, 15, 20, and 28 May are highlighted by solid circles and are accompanied by rings which represent the extent of the surface expression of warm water associated with the eddy on those days. Sea surface height anomaly centers for 3, 10, 17, and 24 May are denoted by solid diamonds, with lines representing interim periods. (b) Daily estimate of the ratio of the east-west and north-south extent of the eddy, calculated from sea surface temperature images, using the 22°C contour as an eddy boundary.

near the coastal region. However, by the end of the study period, when in deep ocean waters, there was close agreement (14 km difference) in the location of the eddy center derived from SST and SSHA.

[17] Shortly after the cruise (6 June 2006), Alpha had shifted about 100 km southward and its connection with the LC and shelf waters became tenuous (Figures 4a, 4c, and 4e). At this time, its distinct circular sea surface height anomaly was lost, either because of a change in its physical properties or because of not being fully resolved by altimeter along-track data. It remained in this state until mid-June, when the LC injected new water into its warm center. The eddy intensified and interacted with another anticyclonic eddy to its north. At this time a pool of warm, chlorophyll *a* rich water extends from the shelf out into the ocean. Alpha became dynamically detached from the LC by 18 July (as determined from altimeter data), with its center at 33.5°S 112.5°E. However, a weaker linkage with the LC and shelf waters still appeared to exist in the SST and ocean color images (likely to be a surface feature and the altimeter data may not capture this link) (Figures 4d and 4f). By mid-August Alpha had drifted further westward and the chlorophyll *a* content was depleted (not shown).

3.3. Horizontal and Vertical Circulation

[18] Both multivariate analyses clearly indicated the location and structure of Alpha and the horizontal current speeds associated with Alpha were up to 1 m s^{-1} at 50 as well as 150 m depth (Figure 6), which were consistent with the tangential velocity from the ADCP measurement (Figure 7). Strong vertical shears of horizontal velocity were observed near the thermocline depth (Figure 7). During the first period (2–11 May), the 50 m horizontal current was the strongest northeast of Alpha (Figure 6a). In that region the LC flowed southwestward across the shelf break and circulated the eddy (Figure 7b). Nevertheless, some SST images (not shown) indicated the LC water sporadically flowed southward along the shelf break without surrounding the eddy. To the southeast of the eddy, the current split, either circulating the eddy, or flowing southward to rejoin the LC.

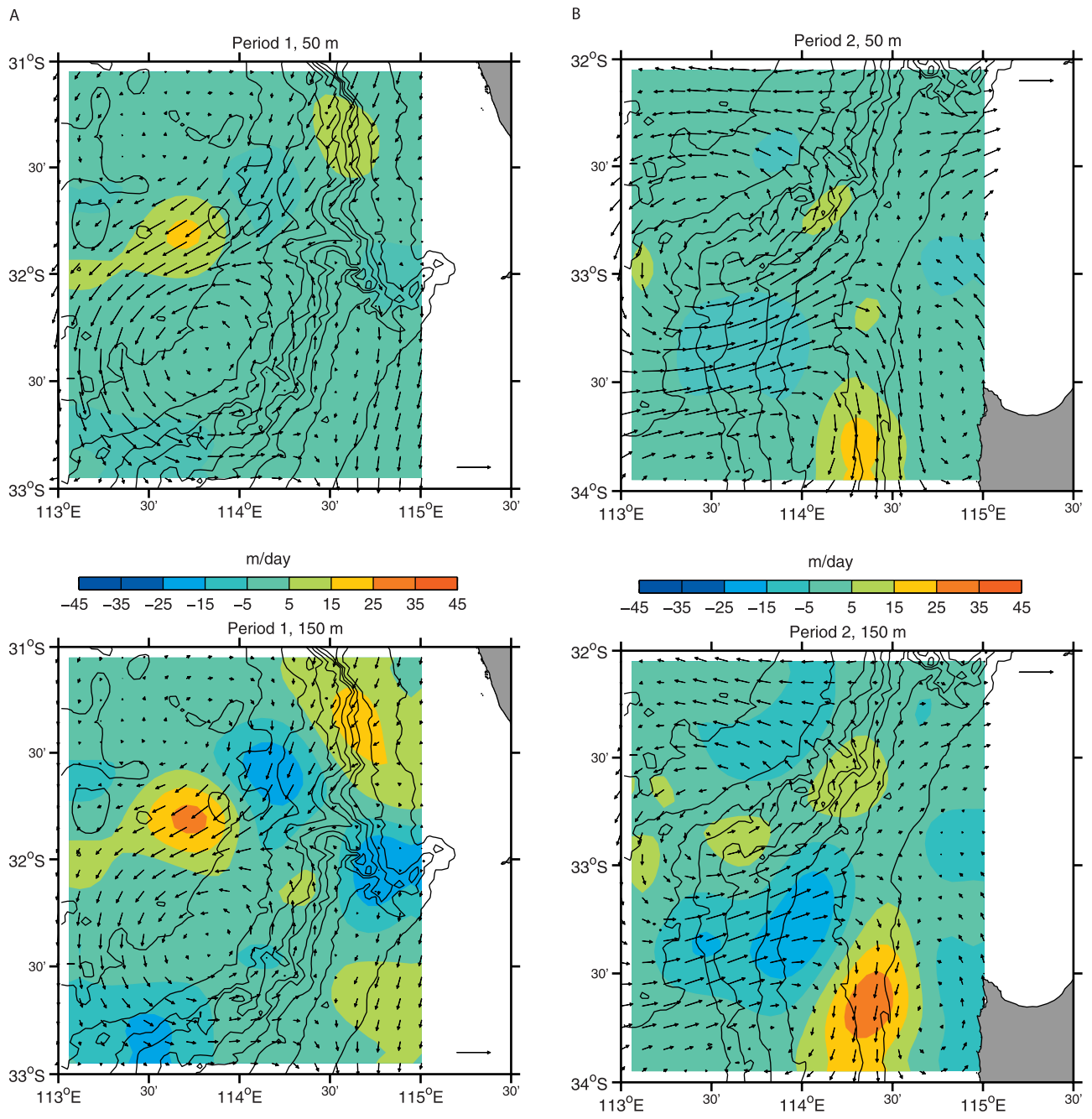

Figure 6. (a) Horizontal and vertical velocities at 50 and 150 m depth obtained from the solution of the multivariate analysis of acoustic Doppler current profiler and CTD data and the subsequent inversion of the quasi-geostrophic Omega equation for Period 1, from 2–11 May 2006, eddy center 113.8°E, 32.25°S. (b) Same as Figure 6a except for Period 2, from 14–25 May 2006, eddy center 113.75°E, 32.7°S. The vectors at the bottom right of Figure 6a or top right of Figure 6b denote 1 m s^{-1} velocity. The vertical velocities are given by the color code. Lines are depth contours at 500 m intervals. The horizontal velocities are plotted at every other grid point.

[19] The main regions of up and down welling were located along the high-velocity flow surrounding the eddy. Vertical motions were stronger at 150 m than 50 m. The maximum upwelling values were 25–35 m d^{-1}, at 150 m depth near the northern boundary of Alpha. Maximum down welling values of 15–25 m d^{-1} were recorded in three locations around the eddy. Where the LC flowed across the shelf break into the ocean there was local upwelling of 5–15 m d^{-1} at 50 m and of 15–25 m d^{-1} at 150 m depth. This confirms the suggestion of *Feng et al.* [2007] that upward motion along isopycnals is induced by currents flowing offshore across the shelf break. Near the eddy center, the vertical motion was mostly negligible.

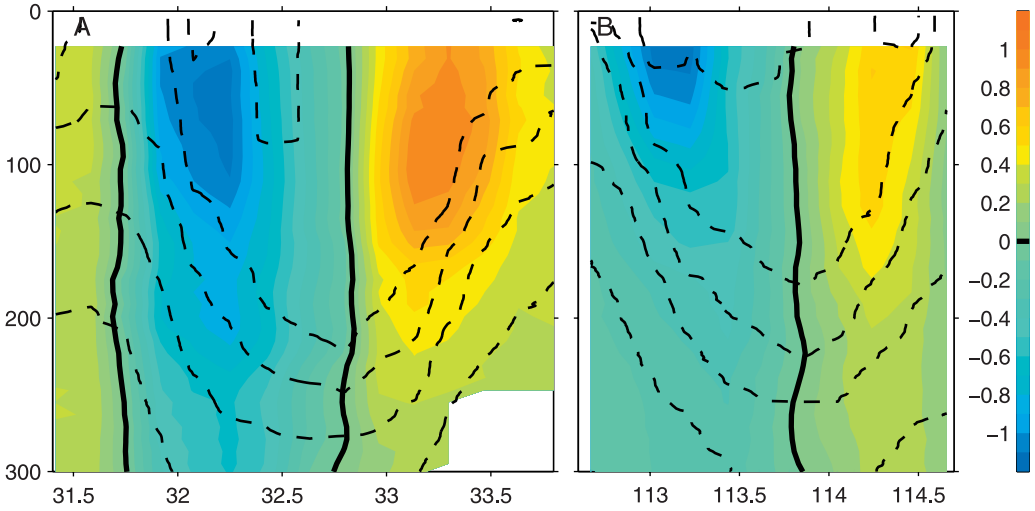

Figure 7. (a) Zonal velocity along a north-south transect conducted at 113.6E (21–23 May 2006) and (b) meridional velocity along a west-east transect at 32.3S (8–9 May 2006), as shown in Figure 1. Isopycnals are plotted as dashed lines at 0.5 kg m^{-3} interval.

[20] During the second period (14–25 May), the station distribution does not appear to have captured the LC to the north of Alpha (Figure 6b). Unlike the first period, the center of the eddy showed some upward motion of between 5–15 m d^{-1}. Downwelling values of the order of 15–25 m d^{-1} were to the southeast side of the eddy, and the strongest upwelling was to the southeast of the major downwelling area where the LC moved inshore across the shelf break.

[21] SST images (not shown) revealed that a tongue of subtropical front water, originating from the south, often extended around the southeastern side of Alpha. This tongue developed during the first 9 days of the cruise and was eventually pinched off to form a distinct cool cell, as seen in the SST image on May 10 (Figure 3c). The location of the initial cool cell coincided with a cyclonic eddy (Beta) identified by the Omega equation analysis (Figure 6a). In the second period, Beta was weaker and had moved a few kilometers northeastward. Note that the rotation of Beta was not evident from Aviso SSHA data.

3.4. Water Mass Properties

[22] The contours of the temperature follow a bowl shape below the surface mixed layer, consistent with the baroclinic structure of Alpha. The bowl shape of Alpha was also clearly defined by the salinity maximum water (Figure 8), below which there was a decrease in temperature and salinity. There was a weak deepening trend ($P < 0.01$) of the mixed layer toward the center of Alpha (Figure 9b).

[23] The lowest-salinity and highest-temperature signature in the surface mixed layer was observed in a north-south transect at 32.1°S in the LC during period 2, coinciding with a shallow mixed layer (~50 m). During period 1, a similar feature can be seen on the west-east transect, at 113°E and 114.4°E (Figures 8a and 8c). It is not clear whether they are the same water mass that had circulated within the eddy.

[24] The mixed layer temperature-salinity relationship (Figure 10) showed no clear separation between the LC water and the water mass from the continental shelf. The T-S relationship within these waters is approximately linear, with increasing salinity corresponding to decreasing temperature. Such a relationship might be due to surface air-sea fluxes and mixing and is opposite to the relationship obtained for waters outside of the LC.

[25] The dissolved oxygen concentration was not evenly distributed across the eddy (Figure 8). There was a peak in oxygen concentrations (> 300 μmol L^{-1}) at the surface near the southern boundary of the eddy. Within the eddy, between the salinity maximum and the mixed layer depths, oxygen concentration was as low as 190 μmol L^{-1}. The oxygen concentration below 250 m increased slightly, although just below the salinity maximum it remained lower than the surrounding waters.

3.5. Heat Flux

[26] During the study period the average heat loss to the atmosphere for the eddy was greater (70 W m^{-2}) than for the open ocean at the same latitude, from the NCEP reanalysis data (Figure 11). This is presumably due to fact that the absolute temperature difference between the sea surface and the atmosphere is larger over the LC and forming eddy (114.3°E) than for the cooler open ocean water (110.6°E). The passage of frontal systems (14 and 22 May, Figure 2) across this region appeared to increase the heat flux rate because of lower air temperatures, particularly over the anticyclonic eddy.

3.6. Nutrient Structure

[27] Nitrate was found in relatively high concentrations above the salinity maximum layer near the center of the eddy. The main pool of nitrate (above the salinity maximum) was located near the base of the mixed layer below the photic zone (Figure 12). To estimate the mean and maximum values of this pool, nitrate data between 100–200 m depth from all "center" stations and casts 41–46 and 113–122 were used. This pool had a maximum nitrate concentration of 2.0 μmol L^{-1}, with an average of ~0.9 μmol L^{-1}. The highest silicate concentrations (~4 μmol L^{-1}) were near the center of the eddy (Figure 12c)

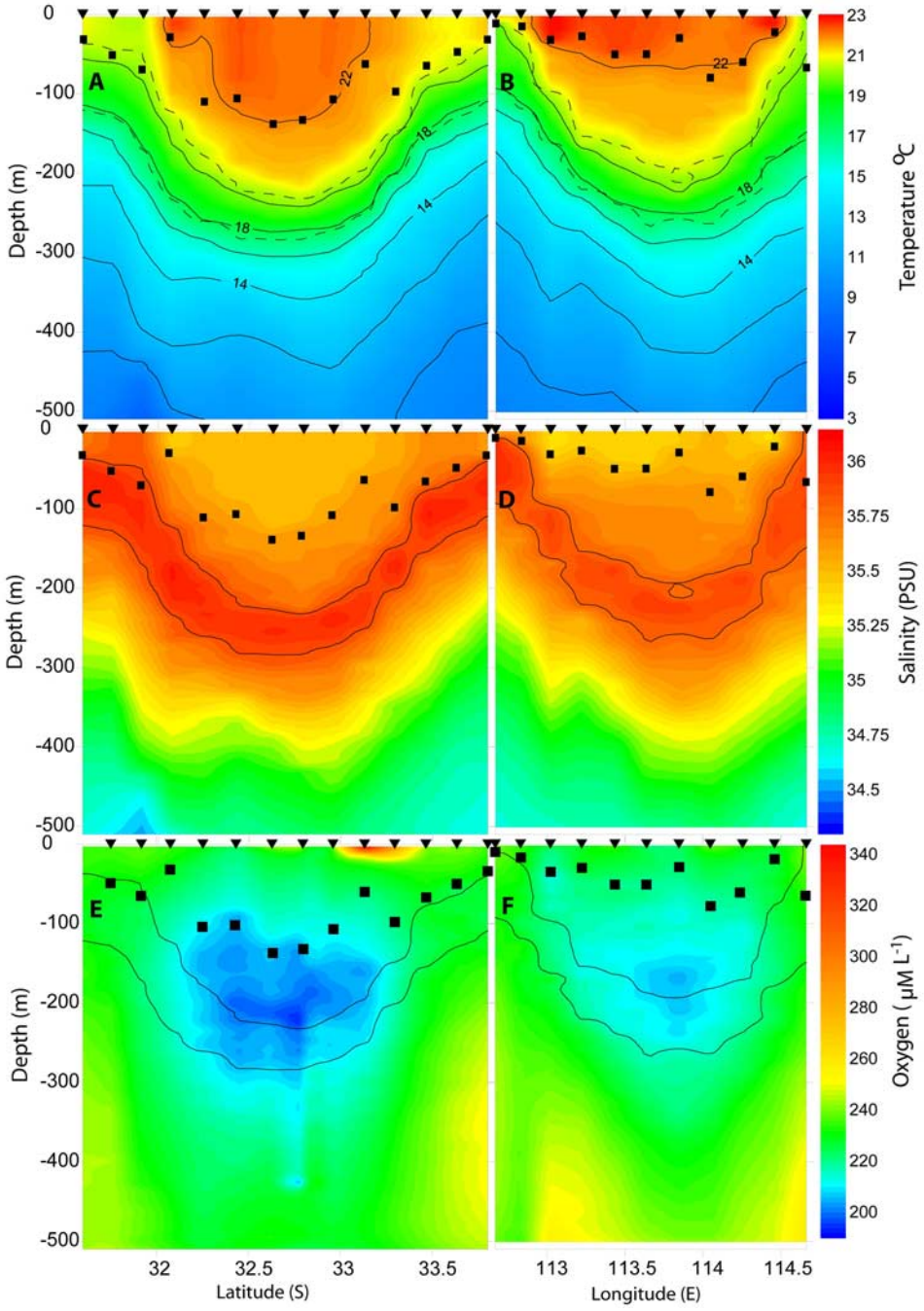

Figure 8. Same as Figure 7, but for the (a, b) temperature, (c, d) salinity, and (e, f) oxygen vertical structures along two transects crossing Alpha. Isotherms are marked in solid lines in Figures 8a and 8b with the 35.8 salinity contour marked by the dashed line. In Figures 8c, 8d, 8e, and 8f the 35.8 salinity contour is marked by a solid line. The locations of CTD casts are identified by triangles at the top of each panel, and squares denote the depth of the mixed layer.

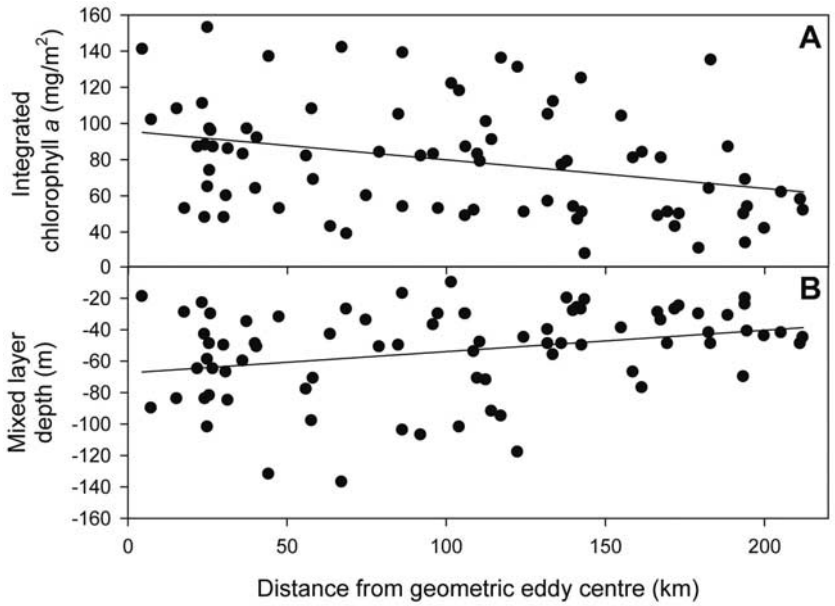

Figure 9. (a) Radial distribution of the 0–200 m integrated chlorophyll *a* biomass integrated chlorophyll *a* ($r^2 = 0.10$). (b) Radial distribution of the mixed layer depth ($r^2 = 0.08$).

with the remainder of the eddy having concentrations near 3 μmol L^{-1}, slightly less than that reported by *Lourey et al.* [2006] for the LC. Silicate concentrations of ~3 μmol L^{-1} extended into the salinity maximum. Silicate level diminished immediately below this layer.

3.7. Fluorescence Structure

[28] Fluorescence was significantly correlated with chlorophyll *a* concentration ($P < 0.001$). Fluorescence was not evenly distributed across the eddy. To the north of the eddy (Figure 12e), the bottom of the mixed layer coincided with a deep chlorophyll *a* maximum (DCM), but this signal was lost at the outer perimeter of the eddy (32.1°S) (Figure 12e). The fluorescence distribution in the northern half of the eddy was horizontally patchy, possibly resulting from interleaving between shelf, LC and recirculated eddy water filaments. The southern half of the eddy had a high fluorescence signal from the surface to the bottom of the mixed layer. The eastern and western peripheries of the eddy (Figure 12f) had established DCM, while the mid section of the eddy had chlorophyll *a* concentrations evenly distributed within the mixed layer.

4. Discussion

4.1. Water Mass

[29] One of the overriding premises in previous works [e.g., *Pearce and Griffiths*, 1991; *Moore et al.*, 2007] has been that eddy water originates from the shelf environment. However, this is not clearly evident in TS plots from this (Figure 10) or previous studies [*Morrow et al.*, 2003; *Feng et al.*, 2007] because of the pervasive regional influence of the LC, which may supply water to forming eddies both in a direct way and indirectly via supply of the shelf regions. Long-term investigations of shelf region off the southwestern Australia have indicated that the LC may periodically flood the shelf [*Pearce et al.*, 2006; *Koslow et al.*, 2008], resulting in a typical LC signature appearing both on the shelf, and in the forming eddy. But a distinction between shelf and LC waters may be made from a comparison of the pelagic biota in the water masses. During its formation Alpha may have obtained its initial phytoplankton population from the shelf, but we cannot determine the amount of coastal material transported or if it was a continuous or pulsating connection. The use of time-dependent tracers such as larvae of native, neritic fishes [*Muhling et al.*, 2007, 2008] and numerical simulations can be useful in determining the timing of the exchanges between the shelf and forming eddies.

[30] The water column structure was similar to that described by *Morrow et al.* [2003] for another eddy in the eastern Indian Ocean. They determined that the surface layers were strongly influenced by the low-density waters of the LC, which flowed over a layer of Subtropical Surface Water, represented by a salinity maximum (>35.6) [*Morrow et al.*, 2003]. *Warren* [1981] suggested that the salinity maximum was due to evaporation exceeding precipitation at latitudes 25°S–35°S. This water may then be subducted under the Leeuwin Current [*Waite et al.*, 2007b]. *Warren* [1981] also found an oxygen minimum embedded in the salinity maximum at 18°S. Subsequent to this, *Woo et al.* [2008] have documented that along the 1000 m isobath off the Western Australian coast, the oxygen minimum layer moved upward relative to the salinity maximum from south to north. Within the bowl of Alpha the oxygen minimum was isolated above the salinity maximum, suggesting some perturbation of the system, either physical or biological.

4.2. Nutrients

[31] The large anticyclonic eddies that form in the eastern boundary of the Indian Ocean tend to be productive, in contrast to anticyclonic eddies elsewhere [*Mizobata et al.*, 2002; *Hormazabal et al.*, 2004; *Crawford et al.*, 2005]. Previous investigations of LC eddies have hypothesized

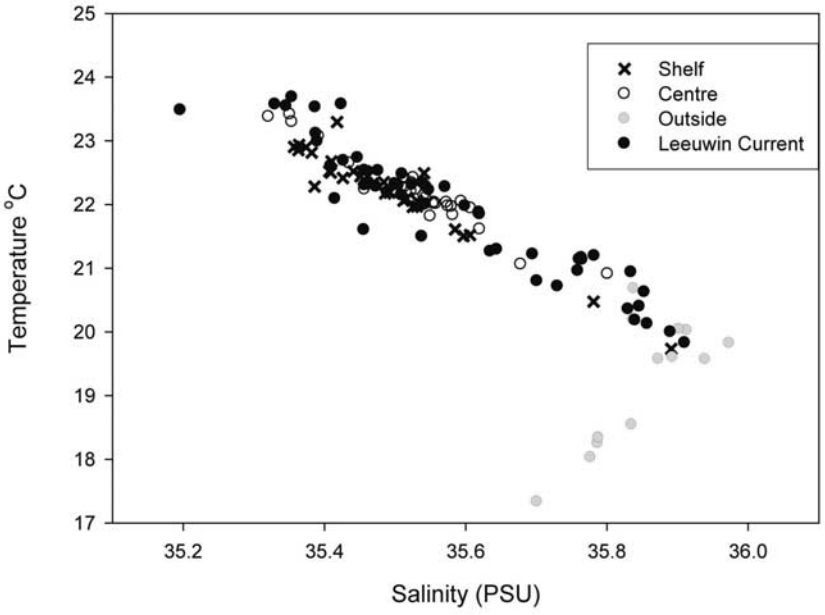

Figure 10. Mixed layer temperature-salinity relationship derived from CTD data during the May 2006 cruise. Multiplication signs show stations from shallow water. Open circles show stations located in center of eddy. Closed gray circles show stations in cool oceanic water. Closed black circles show stations from within the Leeuwin Current.

[*Waite et al.*, 2007a] that nutrients are incorporated into LC eddies during their formation making them fertile enough to support large phytoplankton populations. The high level of nitrate found in the forming 2006 eddy supports this hypothesis. Presumably a developing eddy, seeded with coastal, shelf and LC phytoplankton would represent an environment where only suitably adaptable species would persist. In the case of the mature 2003 eddy those species included diatoms capable of undertaking extensive vertical migration.

[32] Within the forming eddy, the nitrate pool had an average nitrate concentration almost double the regional value of 0.5 μmol L^{-1} suggested by *Lourey et al.* [2006] for the shelf and LC waters. The likely sources of nitrate in the eddy have not yet been clearly identified, although it is unlikely to be from regional surface waters [*Lourey et al.*, 2006]. Downwelling is due to the convergence nature of the poleward flowing LC [*Feng et al.*, 2007], however, the eddy motion interacting with the continental slope and shelf break has been identified as a potential mechanism for upwelling [*Feng et al.*, 2007]. The strong shear between the LC and the underlying water, combined with convective mixing driven by heat loss as the LC travels southward, may entrain nutrients from the shelf.

[33] Cyclonic eddies, such as Beta, may be another source of nutrients, as they potentially upwell nutrient rich water of the Leeuwin Undercurrent. The location of Beta is identical to the location of cyclonic eddies modelled by *Rennie et al.* [2007] to elucidate the influence of the Perth Canyon on regional currents. They found that these eddies were transient, and detected six distinct reoccurring patterns of eddies. If these geographically constrained eddies are transient, but reoccurring they may be important components in the development and nutrient dynamics of anticyclonic eddies, through eddy-eddy interaction. It has been noted previously by *Levy et al.* [2001] and *Waite et al.* [2007b] that submesoscale processes ($\sim$5–20 km) in the periphery of anticyclonic eddies can play a critical role in the supply of nutrients, distribution of phytoplankton and levels of new production.

[34] One primary biological source of nitrate in the anticyclonic eddy could be in situ nitrification [*Libes*, 1992]. *Warren* [1981] suggested that the oxygen minimum may be the result of oxygen consumption or respiration below the photic zone and that demineralization may account for the relatively high levels of nutrients found at that depth. Given the findings of *Warren* [1981] and the

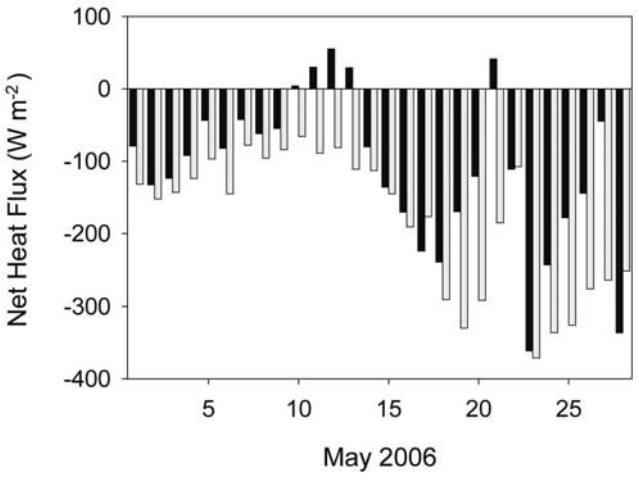

Figure 11. Daily average net air-sea heat flux from National Center for Environment Prediction reanalysis during May 2006 for (black) longitude 110.6°E and (gray) 114.3°E. Positive values denote net heat inputs into the ocean across the air-sea interface.

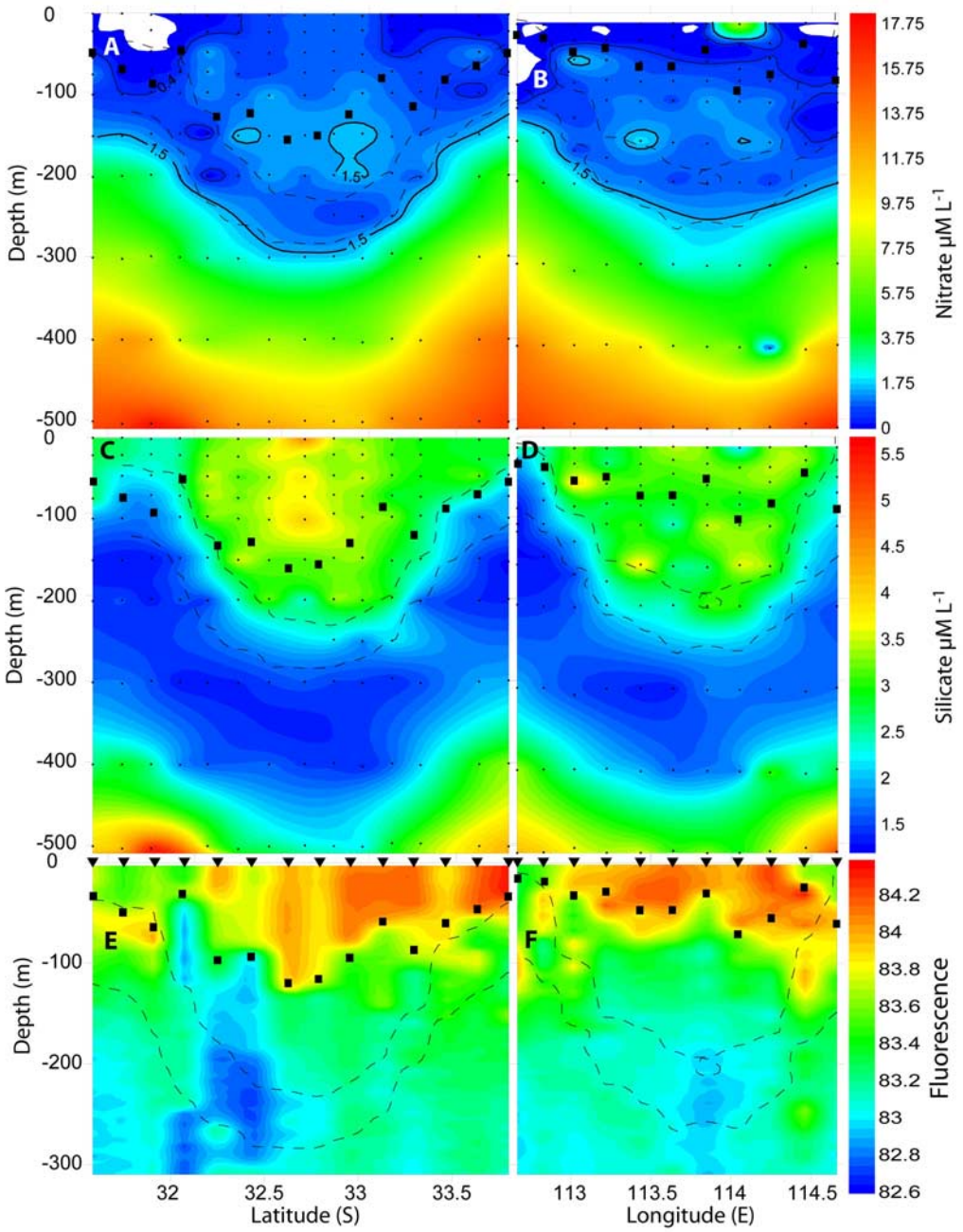

Figure 12. Same as Figures 7 and 8, except for (a, b) vertical nitrate, (c, d) silicate, and (e, f) fluorescence (relative units) distributions along two transects crossing Alpha off southwestern Australia. The 35.8 salinity contour is marked by a dashed line in all panels. Sample locations are identified by black dots in Figures 12a, 12b, 12c, and 12d. In Figures 12a and 12b the 1.5 μmol contour is marked by a heavy black line, the 0.4 μmol contour is marked by a light black line, and the regions where nitrate levels were below detection are white. Squares denote the depth of the mixed layer, and the locations of CTD casts are identified by triangles at the top of Figures 12e and 12f. The near-surface high nitrate value near 114°E in Figure 12a may be erroneous.

location of the oxygen minimum below both the mixed layer and photic zone, we suggest that this region is potentially net heterotrophic, with many of its community members rematerializing sinking material. It is possible that nitrification is occurring in this layer of water, the result of the thermocline presenting a barrier to export flux and the position of this process indicated by an oxygen minimum and nitrate maximum. This biological process could affect a more continuous supply of nitrate than transient physical upwelling processes. In addition, the low oxygen signal above the salinity maximum in the center of the eddy could represent the net effect of nitrification processes.

[35] The bulk of the nitrate was found to be immediately below the mixed layer suggesting that time-dependent

deepening of the mixed layer might allow nitrate to be gradually mixed into the photic zone. Such a slow release of nutrients into the photic zone may allow time for the sustained growth of appropriately adapted phytoplankton species of coastal origin, similar to those found in the 2003 eddy [*Thompson et al.*, 2007], to out-compete other species to become established in anticyclonic eddies.

[36] As the distribution of silicate surrounding, and within, the forming eddy differed significantly from that of nitrate, we suggest that these nutrients are subject to different physical and biological distribution processes. The high silicate concentrations in the center of the eddy may indicate the potentially convergent nature of the eddy but the origin and form of that material can only be speculated upon. The ambient silicate concentration in the eddy was slightly lower than for the LC [*Lourey et al.*, 2006], suggesting potential dilution of the LC by silicate-poor, shelf waters within the eddy. Regional upwelling of silicate is unlikely because of the wide (~200 m) silicate depleted layer under the salinity maximum. Other sources of silica-rich water include the intrusions of Subtropical Frontal water from the southeast side of the eddy and advection of silica rich particles, such as diatom frustules, into the eddy from the shelf.

4.3. Comparison With 2003 Mature Eddy

[37] The physical structure of the mature 2003 anticyclonic eddy studied by *Feng et al.* [2007], and the forming eddy in 2006 (this study) were generally similar, but some differences relating to age and interactions with other oceanographic features were found. For example, both eddies had a distinct bowl shape defined by the depth of the mixed layer, although the mixed layer of the mature eddy was deeper (275 m) than the forming eddy (140 m). The temperature and salinity signatures in the core of each eddy deepened toward the center, although the absolute values differed: the forming eddy was warmer by ~4°C and less salty (0.2 PSU). The continued addition of warm water into the 2006 eddy presumably maintained the substantial loss of heat to the relatively cool atmosphere.

[38] The higher salinity values in the mature (2003) eddy are likely to have been caused by evaporation and mixing with more saline oceanic water. In 2006, the forming eddy had a salinity of 35.53 and the oceanic waters 35.81, whereas the mature 2003 eddy had a salinity of 35.7. If dilution was the only mechanism changing the salinity, and the eddy remained the same size, then ~60% of its water would have needed to have been exchanged with oceanic water. However, this is clearly an overestimation as evaporation and entrainment of other water masses would also have influenced the temperature and salinity signatures. 2006 is an El Niño year so that the LC is weaker compared to 2003 [*Feng et al.*, 2003], which may cause the fact that the 2006 eddy was less persistent compared with the 2003 eddy, likely because of the less eddy energy derived from the LC [*Feng et al.*, 2005].

5. Summary

[39] In this study, the physical and chemical signatures of a developing anticyclonic eddy from the Leeuwin Current off the west coast of Australia were analyzed using data from both an R/V *Southern Surveyor* cruise during May 2006 and satellite observations during the life time of the eddy. The main results from this study are summarized: (1) the R/V *Southern Surveyor* cruise captured the main physical and chemical features of the developing eddy; (2) strong cross-shelf exchanges were observed during the eddy formation, and the water masses within the eddy were mainly derived directly from the Leeuwin Current or modified Leeuwin Current water on the shelf; (3) near the center of the eddy, high nitrate concentrations (up to 2 μmol L^{-1}) were observed just below the mixed layer depth, and high silicate concentrations (up to 4 μmol L^{-1}) were observed within the mixed layer; (4) the source of the nutrients within the eddy may be due to physical disturbances by the Leeuwin Current and eddy-eddy interaction or due to nitrification process; and (5) the relative high levels of nutrients could provide a suitable environment for diatoms/phytoplankton to bloom within the eddy at a later stage of eddy evolution.

[40] **Acknowledgments.** We acknowledge ARC discovery grant 2006–2008 to Anya Waite and Strategic Research Fund for the Marine Environment (SRFME) Collaborative Grant to Anya Waite, P. A. Thompson, and L. Twomey. Ming Feng and David Holliday are also supported by the Western Australian Marine Science Institution. We thank the Marine National Facility for ship time and the staff and crew of the R/V *Southern Surveyor*. We also thank all colleagues who participated in the voyage and those who worked ashore, especially Lindsay Pender from CSIRO.

References

Crawford, W. R., P. J. Brickley, T. D. Peterson, and A. C. Thomas (2005), Impact of Haida eddies on chlorophyll distribution in the eastern Gulf of Alaska, *Deep Sea Res., Part II*, *52*, 975–989, doi:10.1016/j.dsr2.2005.02.011.

Cresswell, G. R., and T. J. Golding (1980), Observations of a south-flowing current in the southeastern Indian Ocean, *Deep Sea Res. Part A*, *27*, 449–466, doi:10.1016/0198-0149(80)90055-2.

Ducet, N., P. Y. LeTraon, and G. Reverdin (2000), Global high resolution mapping of ocean circulation from TOPEX/Poseidon and ERS-1/2, *J. Geophys. Res.*, *105*, 19,477–19,498, doi:10.1029/2000JC900063.

Feng, M., G. Meyers, A. Pearce, and S. Wijffels (2003), Annual and interannual variations of the Leeuwin Current at 32°S, *J. Geophys. Res.*, *108*(C11), 3355, doi:10.1029/2002JC001763.

Feng, M., S. Wijffels, J. S. Godfrey, and G. Meyers (2005), Do eddies play a role in the momentum balance of the Leeuwin Current?, *J. Phys. Oceanogr.*, *35*(6), 964–975, doi:10.1175/JPO2730.1.

Feng, M., L. J. Majewski, C. B. Fandry, and A.M Waite (2007), Characteristics of two counter-rotating eddies in the Leeuwin Current system off the Western Australian coast, *Deep Sea Res., Part II*, *54*, 961–980, doi:10.1016/j.dsr2.2006.11.022.

Gomis, D., and M. A. Pedder (2005a), Errors in dynamical fields inferred from synoptic oceanographic cruise data. Part I: The impact of observation errors and the sampling distribution, *J. Mar. Syst.*, *56*(3–4), 317–333, doi:10.1016/j.jmarsys.2005.02.002.

Gomis, D., and M. A. Pedder (2005b), Errors in dynamical fields inferred from synoptic oceanographic cruise data. Part II: The impact of the lack of synopticity, *J. Mar. Syst.*, *56*(3–4), 334–351, doi:10.1016/j.jmarsys.2005.02.003.

Gomis, D., S. Ruiz, and M. A. Pedder (2001), Diagnostic analysis of the 3D ageostrophic circulation from a multivariate spatial interpolation of CTD and ADCP data, *Deep Sea Res. Part I*, *48*, 269–295, doi:10.1016/S0967-0637(00)00060-1.

Greenwood, J. E., M. Feng, and A. M. Waite (2007), A one-dimensional simulation of biological production in two contrasting mesoscale eddies in the south eastern Indian Ocean, *Deep Sea Res., Part II*, *54*, 1029–1044, doi:10.1016/j.dsr2.2006.10.004.

Griffin, D. A., J. L. Wilkin, C. F. Chubb, A. F. Pearce, and N. Caputi (2001), Ocean currents and the larval phase of Australian western rock lobster, *Panulirus Cygnus, Mar. Freshwater Res.*, *52*, 1187–1199, doi:10.1071/MF01181.

Holton, J. R. (1992), An Introduction to Dynamic Meteorology, 511 pp. Academic, New York.

Hormazabal, S., S. Núñez, D. Arcos, F. Espindola, and G. Yuras (2004), Mesoscale eddies and the pelagic fishery off central Chile (33–40°S), *Gayana (Zool.)*, *68*(2), 291–296.

Kalnay, E., et al. (1996), The NCEP/NCAR 40-year reanalysis project, *Bull. Am. Meteorol. Soc.*, *77*(3), 437–471, doi:10.1175/1520-0477(1996)077<0437:TNYRP>2.0.CO;2.

Koslow, J. A., S. Pesant, M. Feng, A. F. Pearce, P. Fearns, T. Moore, R. Matear, and A. Waite (2008), Structure and dynamics of the pelagic ecosystem off southwestern Western Australia, 2002–2004: Phytoplankton biomass and productivity, *J. Geophys. Res.*, doi:10.1029/2007JC004102, in press.

LeTraon, P. Y., F. Nadal, and N. Ducet (1998), An improved mapping method of multi-satellite altimeter data, *J. Atmos. Oceanic Technol.*, *15*, 522–534, doi:10.1175/1520-0426(1998)015<0522:AIMMOM>2.0.CO;2.

Levy, M., P. Klein, and A. M. Treguier (2001), Impact of sub-mesoscale physics on production and subduction of phytoplankton in an oligotrophic regime, *J. Mar. Res.*, *59*(4), 535–565, doi:10.1357/002224001762842181.

Libes, S. M. (1992), *An Introduction to Marine Biogeochemistry*, 733 pp., John Wiley, New York.

Lourey, M. J., J. R. Dunn, and J. Waring (2006), A mixed-layer nutrient climatology of Leeuwin Current and Western Australian shelf waters: Seasonal nutrient dynamics and biomass, *J. Mar. Syst.*, *59*(1–2), 25–51, doi:10.1016/j.jmarsys.2005.10.001.

Mizobata, K., S. I. Saitoh, A. Shiomoto, T. Miyamura, N. Shiga, K. Imai, M. Toratani, Y. Kajiwara, and K. Sasaoka (2002), Bering Sea cyclonic and anti-cyclonic eddies observed during summer 2000 and 2001, *Prog. Oceanogr.*, *55*, 65–75, doi:10.1016/S0079-6611(02)00070-8.

Moore, T., R. J. Matear, J. Marra, and L. Clementson (2007), Phytoplankton variability off the Western Australian coast: Mesoscale eddies and their role in cross-shelf exchange, *Deep Sea Res., Part II*, *54*, 943–960, doi:10.1016/j.dsr2.2007.02.006.

Morrow, R., F. Fang, M. Fieux, and R. Molcard (2003), Anatomy of three warm-core Leeuwin Current eddies, *Deep Sea Res. Part II*, *50*, 2229–2243, doi:10.1016/S0967-0645(03)00054-7.

Muhling, B. A., L. E. Beckley, and M. P. Olivar (2007), Ickthyoplankton assemblage structure in two mesoscale Leeuwin Current eddies, eastern Indian Ocean, *Deep Sea Res., Part II*, *54*, 1113–1128, doi:10.1016/j.dsr2.2006.05.045.

Muhling, B. A., L. E. Beckley, J. A. Koslow, and A. F. Pearce (2008), Larval fish assemblages and water mass structure off the oligotrophic south-western Australian coast, *Fish. Oceanogr.*, *17*(1), 16–31.

Pearce, A. F., and R. W. Griffiths (1991), The mesoscale structure of the Leeuwin Current: A comparison of laboratory model and satellite images, *J. R. Soc. West. Aust.*, *74*, 35–46.

Pearce, A. F., M. J. Lynch, and C. Hanson (2006), The Hillarys transect (1): Seasonal and cross shelf variability of physical and chemical water properties off Perth, Western Australia, 1996–98, *Cont. Shelf Res.*, *26*, 1689–1729, doi:10.1016/j.csr.2006.05.008.

Rennie, S. J., C. P. Pattiaratchi, and R. D. McCauley (2007), Eddy formation through the interaction between the Leeuwin Current, Leeuwin Undercurrent and topography, *Deep Sea Res., Part II*, *54*, 818–836, doi:10.1016/j.dsr2.2007.02.005.

Thompson, P. A., S. Pesant, and A. M. Waite (2007), Contrasting the vertical differences in the phytoplankton biology of a dipole pair of eddies in the south-eastern Indian Ocean, *Deep Sea Res., Part II*, *54*, 1003–1028, doi:10.1016/j.dsr2.2006.12.009.

Twomey, L. J., A. M. Waite, V. Pez, and C. B. Pattiaratchi (2007), Variability in nitrogen uptake and fixation in the oligotrophic waters off the south west coast of Australia, *Deep Sea Res., Part II*, *54*, 925–942, doi:10.1016/j.dsr2.2006.10.001.

Waite, A. M., et al. (2007a), The Leeuwin Current and its eddies: An introductory overview, *Deep Sea Res., Part II*, *54*, 789–796, doi:10.1016/j.dsr2.2006.12.008.

Waite, A. M., B. A. Muhling, C. M. Holl, L. E. Beckley, J. P. Montoya, J. Strzelecki, P. A. Thompson, and S. Pesant (2007b), Food web structure in two counter-rotating eddies based on δ^{15}N and δ^{13}C isotopic analyses, *Deep Sea Res., Part II*, *54*, 1055–1075, doi:10.1016/j.dsr2.2006.12.010.

Warren, B. A. (1981), Trans-Indian hydrographic section at Lat. 18(S: Property distributions and circulation in the South Indian Ocean, *Deep Sea Res., Part A*, *28*, 759–788.

Woo, M., C. B. Pattiaratchi, and W. W. Schroeder (2008), Hydrography and water masses off the West Australian Coast, *Deep Sea Res., Part I*, doi:10.1016/j.dsr.2008.05.005, in press.

L. E. Beckley and D. Holliday, School of Environmental Science, Murdoch University, 90 South Street, Murdoch, WA 6150, Australia.

M. Feng, CSIRO Marine and Atmospheric Research, Private Bag 5, Wembley, WA 6913, Australia. (ming.feng@csiro.au)

D. Gomis, Institut Mediterrani d'Estudis Avançats, UIB-CSIC, E-07190 Esporles, Spain.

H. L. Paterson and A. M. Waite, School of Environmental Systems Engineering, University of Western Australia, Nedlands, WA 6009, Australia.

P. Thompson, CSIRO Marine and Atmospheric Research, GPO Box 1538, Hobart, Tas 7001, Australia.